Harmonic Characteristics Analysis of PWM-Based Electric Vehicle Chargers Considering Control Strategy

Tong Ding, Hongkun Chen, Bin Wu, Pan Hu
School of Electrical Engineering, Wuhan University
Wuhan, China
Email: dingtong@whu.edu.cn

***Abstract*—On the basis of the introduction to the topology of PWM-based electric vehicle (EV) chargers considering control strategy, a theoretical analysis of the harmonic generation mechanism is conducted. By establishing simulation models of the charger, the distribution order of characteristic harmonic generated by single charger is analyzed. Furthermore, the harmonic coupling characteristics of multiple chargers working simultaneously are also discussed. The simulation results show that the harmonics generated by single charger mainly consist of high frequency components, including a small amount of low frequency components. As for multiple chargers, with the increase of the number of the chargers and the charging power, each harmonic current ratio and the current total harmonic distortion both show a downward trend.**

***Index Terms*-- control strategy, electric vehicle charger, harmonic analysis, PWM rectifier.**

I. INTRODUCTION

Electric vehicles (EVs) have been widely popularized due to their obvious advantages in mitigating environmental pollution and energy crisis [1]. As the main charging facilities for EVs, EV chargers can be classified into different types according to the rectifier utilized. Diode-controlled rectifier or thyristor phase-controlled rectifier is commonly utilized by EV chargers in the current market. As a result, a large number of harmonics are injected into the power grid during the operation, which affects the safe and stable operation of the power grid [2]. By comparison, the pulse width modulation (PWM) rectifier can be used to effectively mitigate the harmonic generation so that it has a promising prospect. However, the PWM rectifier also brings new harmonic issues, which remain to be further studied.

The researchers have carried out a mass of works on PWM-based EV chargers. Reference [3] has proposed the novel combined application of zero current switch and PMW for EV chargers, which can help to reduce the voltage and current load on the power grid, but the specific characteristics of harmonic generated by the chargers are not analyzed. Reference [4] has discussed the SVPWM-based charger controlled by fuzzy double closed loop, which can reduce the harmonic pollution to the power grid by control of the power factor, but the overall control strategy of the charger is lack of complete and systematic introduction. Reference [5], [6] have established the simulation models to analyze the harmonic effect caused by PWM-based EV chargers connected to the power grid, but the theoretical research on the mechanism of harmonic generation is not conducted.

In order to make out the harmonic characteristics of PWM-based EV chargers, as well as the harmonic coupling characteristics of multiple chargers, a theoretical analysis of the harmonic generation mechanism based on the topology of the chargers considering control strategy is conducted. By establishing a simulation model of single charger, the distribution order of characteristic harmonic is analyzed. When multiple chargers work simultaneously, the variations of each harmonic current ratio and the current total harmonic distortion with the number of the chargers and the charging power are also discussed.

II. TOPOLOGY OF PWM-BASED EV CHARGERS CONSIDERING CONTROL STRATEGY

A. Topology of the Charger

The topology of a PWM-based EV charger is shown in Fig.1, which mainly consists of PWM rectifier and DC/DC power converter. The basic working principle of the charger is that the three-phase AC power from 10kV distribution network is step-down to supply the charger by the transformer, and it is converted to DC power by PWM rectifier in order to provide DC input for DC/DC power converter through the filter circuit, by which the DC voltage is adjusted to an appropriate value to charge the EV battery.

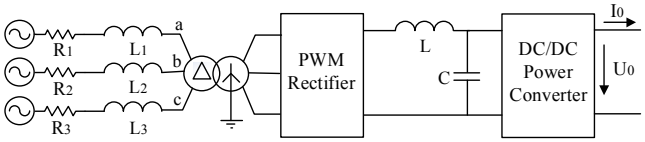

Figure 1. Topology of PWM-based EV charger

978-1-5386-0517-2/18/$31.00 ©2018 IEEE

B. Control Strategy of PWM Rectifier

The EV charger utilizes three-phase voltage-source PWM rectifier, the output voltage of which can be regulated among a certain extent higher than the peak value of the input AC voltage. The bidirectional flow of power can be achieved, and it is possible to make the power factor close to 1, which is beneficial to the realization of vehicle to grid (V2G) [7]. Fig.2 depicts the topology of three-phase voltage-source PWM rectifier.

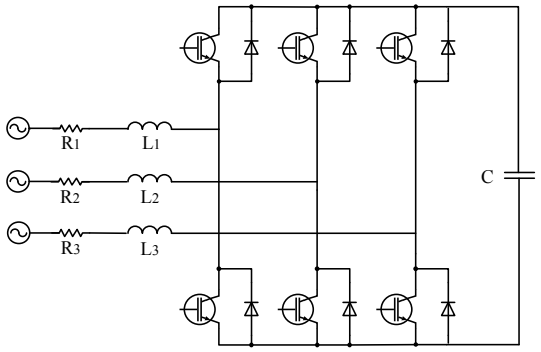

Figure 2. Topology of three-phase voltage-source PWM rectifier

As for the generation of control signals, the rectifier employs the control approach of voltage and current double closed loop based on the dq0 double-phase rotating coordinate system, which can decouple the active and reactive components to achieve the easier manipulation of the output. The double closed loop control consists of voltage outer loop and current inner loop. The function of the former is to maintain the stability of the DC output voltage, and the role of the latter is to regulate the power factor by manipulating the active and reactive components of the current [8]. The algorithm generating the control signals is demonstrated in Fig. 3.

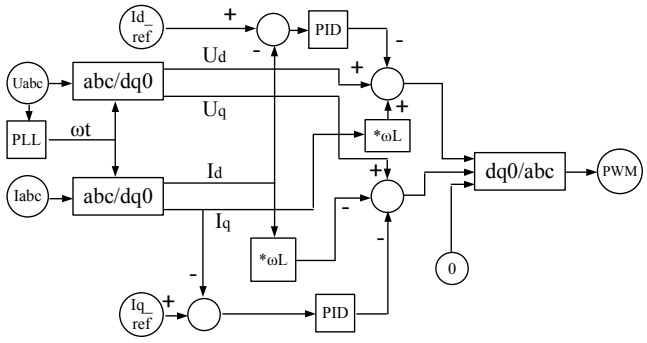

Figure 3. PWM control signal generation flowchart

As shown in Fig.3, the AC voltage and current based on the static three-phase coordinate system are transformed into those based on the rotating double-phase coordinate system, the 0-axis components of which are both omitted. The difference between the given value U_{dc_ref} and the measured value U_{dc} of DC voltage is transformed into the reference value I_{d_ref} of the d-axis component of the current mby a PID controller. The d-axis component U_{do} of the control signal is the sum of the d-axis component U_d of the voltage and the product of I_q and ωL, where I_q refers to the q-axis component of the current and ωL refers to the reactance of the charging inductance L, minus the difference between the d-axis component I_d and its reference value I_{d_ref} of the current processed by a PID controller. The algorithms are displayed in (1) and (2).

$$U_{do} = U_d + \omega L I_q - PID(I_{d\_ref} - I_d) \quad (1)$$

$$I_{d\_ref} = PID(U_{dc\_ref} - U_{dc}) \quad (2)$$

The q-axis component U_{qo} of the control signal is computed by subtracting the q-axis component U_q of the voltage from the product of the d-axis component I_d of the current and the reactance ωL of the charging inductance L, minus the difference between the q-axis component I_q and its reference value I_{q_ref} which can be set to zero of the current, as is demonstrated in (3).

$$U_{qo} = U_q - \omega L I_d - PID(I_{q\_ref} - I_q) \quad (3)$$

The 0-axis component U_{0o} of the voltage can be set to zero. The control signal is converted from the dq0 double-phase rotating coordinate system to the abc three-phase static coordinate system, which is compared with the delta sharp pulse carrier signal to produce the corresponding PWM signal.

C. Control Strategy of DC/DC Power Converter

The EV charger utilizes the bidirectional isolated power converter consisting of the IGBT full bridge controlled by phase shifted signal on both sides, the topology of which is shown in Fig.4.

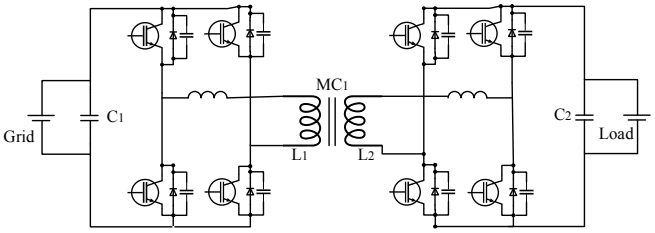

Figure 4. Topology of bidirectional isolated power converter

There are many kinds of control modes between two full bridges, among which the single phase shift control is widely adopted. The basic control strategy is to make the full-bridge phase of the power output side lead that of the power input side, while the phase of the front and rear arm of each full bridge remains the same.

According to [9], the power transmitted in the converter can be obtained by (4).

$$P=\frac{nV_bV_s}{2fL}(D-D^2) \tag{4}$$

Where, P is the transmission power, n is the ratio of the high-frequency transformer, V_b and V_s are the voltage of load and power respectively, f is the frequency of the converter, L is the inductance converted to the primary side of the transformer, and D is the ratio of the phase shift time to the half cycle time.

The transmission power can also be expressed as

$$P=V_sI_s=V_bI_b \tag{5}$$

Both sides of (5) are divided by the load voltage V_b, and the load current I_b can be represented as

$$I_b=\frac{nV_s}{2fL}(D-D^2) \tag{6}$$

D can be obtained by (7), which is derived from (6). According to (7), the phase shift time t_p can be calculated by (8).

$$D=\frac{1\pm\sqrt{1-4\cdot\frac{2fLI_b}{nV_s}}}{2}=\frac{1}{2}\pm\sqrt{\frac{1}{4}-\frac{2fLI_b}{nV_s}} \tag{7}$$

$$t_p=D\cdot\frac{T}{2}=D\cdot\frac{1}{2f}=\frac{1}{4f}+\sqrt{\frac{1}{16f^2}-\frac{LI_b}{2fnV_s}} \tag{8}$$

III. HARMONIC CHARACTERISTICS ANALYSIS OF PWM-BASED EV CHARGERS

A. Harmonic Generation Mechanism

The harmonic generated by three-phase voltage-source PWM rectifier consists of the components of high frequency and low frequency. The high-frequency harmonic is generated by modulation, while the low-frequency harmonic is caused by the dead time.

As for the high-frequency harmonic, the output voltage of each bridge arm is Fourier-developed when the bipolar modulation strategy is adopted, and the fundamental voltage and harmonic voltage of the bridge arm of the rectifier can be calculated according to the superposition principle [10]. The fundamental voltage can be expressed as

$$U_{ab1}=\frac{\sqrt{3}}{2}aU_d\sin(\omega_rt+\varphi) \tag{9}$$

Where, a is the modulation index, U_d is the DC voltage, and ω_r is the angular frequency of the modulation signal.

The harmonic of output line voltage can be represented as follows.

1) When $n=1,3,5,\ldots$, $k=3(2m-1)\pm1$, and $m=1,2,\ldots$, the harmonic voltage can be calculated by (10).

$$\frac{2U_{abh}}{U_d}=\sum_{n=1}^{\infty}(-1)^{\frac{n+1}{2}}(\frac{4}{n\pi})\sum_{k=2}^{\infty}J_k(\frac{an\pi}{2})\times \{\sin[(k\omega_r+n\omega_c)+k(\varphi-\frac{\pi}{3})]- \sin[(k\omega_r-n\omega_c)+k(\varphi-\frac{\pi}{3})]\}2\sin\frac{k\pi}{3} \tag{10}$$

Where, J represents the Bessel function, and ω_c represents the angular frequency of carrier signal.

2) When $n=2,4,6,\ldots$, and $k=\begin{cases}6m+1 & m=0,1,\ldots\\ 6m-1 & m=1,2,\ldots\end{cases}$, the harmonic voltage can be obtained by (11).

$$\frac{2U_{abh}}{U_d}=\sum_{n=1}^{\infty}(-1)^{\frac{n}{2}}(\frac{4}{n\pi})\sum_{k=2}^{\infty}(-1)^kJ_k(\frac{an\pi}{2})\times \{\cos[(k\omega_r+n\omega_c)+k(\varphi-\frac{\pi}{3})]- \cos[(k\omega_r-n\omega_c)+k(\varphi-\frac{\pi}{3})]\}2\sin\frac{k\pi}{3} \tag{11}$$

Based on the above analysis, the amplitude of the harmonic voltage can be expressed as

$$U_h=\frac{U_d}{2}(\frac{4}{n\pi})J_k(\frac{an\pi}{2}) \tag{12}$$

The harmonic angular frequencies are $n\omega_c\pm k\omega_r$.

The harmonic voltage on the bridge arm side causes the distortion of the current on the grid side, the harmonic components of which can be represented as

$$I_{ah}(n)=\frac{U_{abh}(n)}{\omega_n(L_s+L_z)} \tag{13}$$

Where, L_s is the filter inductance, L_z is the inductance on the grid side, and ω_n is the angular frequency corresponding to n order harmonic.

As for the low-frequency harmonic, the harmonic voltage generated by the rectifier can be derived from the error voltage caused by the dead time by Fourier decomposition [11], which can be expressed as

$$U_{abl} = \frac{8 f_c t_d U_d}{n\pi} \sin[n(\omega_r t - \varphi)] \qquad (14)$$

Where, φ represents the initial phase angle of modulation wave, n =3,5,7,9,⋯, f_c represents the carrier frequency, and t_d represents the dead time.

The result of calculation and analysis shows that the angular frequencies of high-frequency harmonics generated by the three-phase voltage-source PWM rectifier are basically $\omega_c \pm 2\omega_r$, $2\omega_c \pm \omega_r$ and $3\omega_c \pm 2\omega_r$, while the main components of low-frequency harmonics consist of the 5th, 7th, 11th and 13th.

B. Harmonic Simulation Analysis

1) Single charger

According to the control strategy proposed above, a simulation model of single PWM-based EV charger is established, where the switching frequency of the PWM rectifier is set to 10kHz, and the system frequency is set to 50Hz. The simulation results of the line voltage on the bridge arm side of the rectifier and the current on the grid side are respectively shown in Fig.5 and Fig.6. It is indicated that the voltage waveform is a series of periodic rectangular wave and the current waveform is close to sine wave, the distortion of which is small.

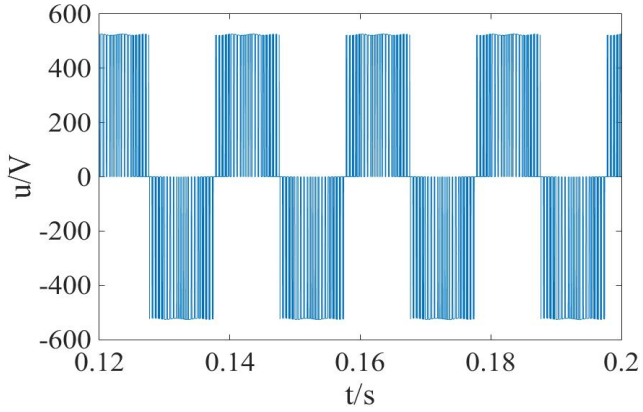

Figure 5. Line voltage waveform on the bridge arm side

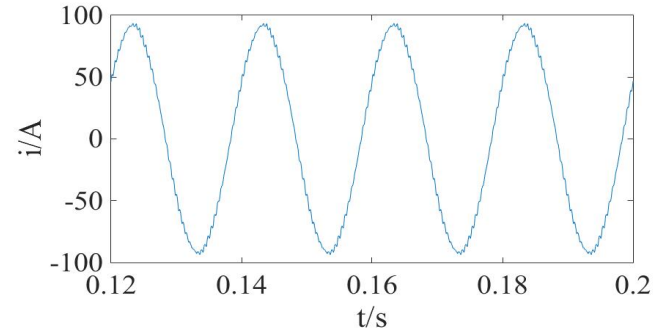

Figure 6. Current waveform on the grid side

The fast Fourier transform (FFT) is utilized to analyze harmonic characteristics of the voltage and current above. The waveform spectrum of both are respectively demonstrated in Fig.7 and Fig.8. By comparison, the harmonic component of the voltage is consistent with that of the current. The angular frequencies of high-frequency harmonics are concentrated in $n\omega_c \pm k\omega_r$, mainly the 198th, 202nd, 399th, 401st, 598th and 602nd harmonic. In addition, as shown in Fig.8, there are less harmonics of the current on the grid side, and the current total harmonic distortion rate is only 2.27%. Further measurements show that the harmonic current also contains low-frequency components, such as the 5th, 7th, 11th and 13th harmonic. Therefore, the simulation results verify the correctness of the theoretical analysis.

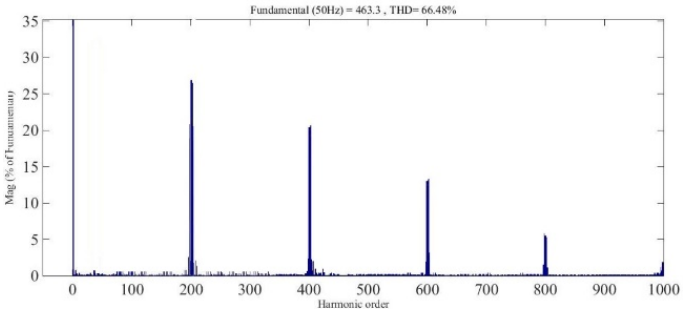

Figure 7. Line voltage waveform spectrum on the bridge arm side

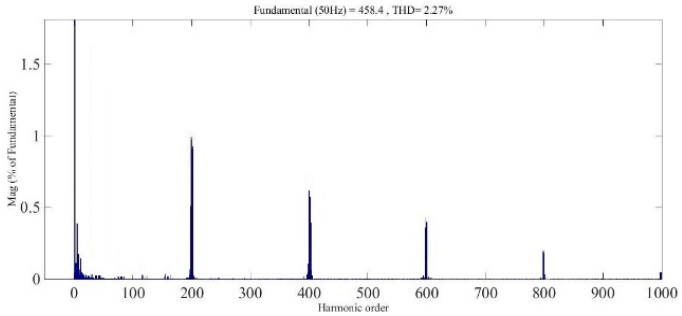

Figure 8. Current waveform spectrum on the grid side

2) Multiple chargers

When multiple chargers work simultaneously, the harmonic current injected into the power grid is not equal to the sum of the harmonic current generated by single charger working alone due to the diversity among the phase angles of harmonic current generated by each charger. The same order harmonic produced by different chargers may cancel each other out, which may make each harmonic current ratio and the current total harmonic distortion decrease with the increase of the number of the chargers.

Fig.9 and Fig.10 depict the variations of the high-frequency and low-frequency harmonics current ratio with the number of the chargers, respectively. Each harmonic current ratio shows a downward trend with the increase of the number of the chargers, which coincides with the conclusion of the theoretical analysis above. In the case of the same number of the chargers, the order of each harmonic current ratio is 198th>202nd>399th>401st>598th>602nd and 5th>7th>11th>13th, that is, in the range of high frequency and low frequency, the higher the harmonic order, the lower the corresponding harmonic current ratio.

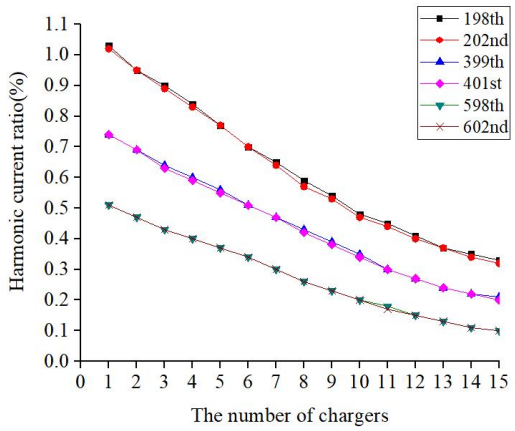

Figure 9. Change in high-frequency harmonics current ratio with the number of the chargers

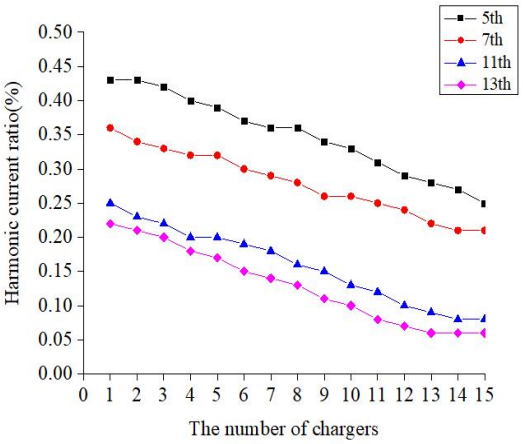

Figure 10. Change in low-frequency harmonics current ratio with the number of the chargers

When the number of the chargers ranges from 1 to 15 and the charging power varies from 10kW to 100kW, the variation of the corresponding current total harmonic distortion is shown in Fig.11, which indicates that the current total harmonic distortion decreases gradually with the increase of the number of the chargers, as well as the higher charging power.

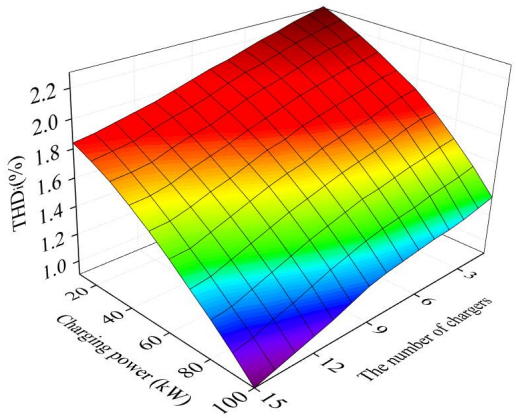

Figure 11. Change in THD_i with the number of the chargers and charging power

IV. CONCLUSION

On the basis of the introduction to the topology of PWM-based EV charger considering control strategy, harmonic characteristics of the charger are discussed by theoretical analysis and simulation, focusing on each harmonic current ratio and the current total harmonic distortion varied with the number of the chargers and the charging power. The main conclusion is summarized as follows.

1) There is low content of harmonics generated by the charger, which mainly consist of high-frequency harmonics, the angular frequencies of which are concentrated in $n\omega_c \pm k\omega_r$, and low-frequency components of the 5th, 7th, 11th and 13th.

2) Each harmonic current ratio shows a downward trend with the increase of the number of the chargers when multiple chargers work simultaneously. In the case of the same number of the chargers, the higher the harmonic order, the lower the corresponding harmonic current ratio in the range of high frequency and low frequency, respectively.

3) The current total harmonic distortion decreases gradually with the increase of the number of the chargers, besides, the downward trend is more obvious with the higher charging power.

REFERENCES

[1] C. H. Dharmakeerthi, N. Mithulananthan, and T. K. Saha. "Modeling and planning of EV fast charging station in power grid," in *2012 IEEE Power & Energy Society General Meeting*, pp. 1-8.

[2] A. Kuperman, U. Levy, J. Goren, A. Zafransky and A. Savernin, "Battery charger for electric vehicle traction battery switch station," *IEEE Trans. Industrial Electronics*, vol. 60, pp. 5391-5399, Dec. 2013.

[3] X. Kong, L. Qin, Y. Wang, J. Zhang, M. Hu and S. Xie. "Lower electric stress ZCS-PWM superbuck converter for electric vehicle DC charging spot," in *2014 International Power Electronics and Application Conference and Exposition*, pp. 754-760.

[4] R. Bai, J. Wan, S. Li and B. Li. "Research on double-close-loop fuzzy controlled SVPWM VSR for EV charger," in *2011 4th International Conference on Power Electronics Systems and Applications*, pp. 1-4.

[5] N. Li and M. Huang. "Analysis on harmonics caused by connecting different types of electric vehicle chargers with power network," Power System Technology. China, vol. 35, pp. 170-174, 2011.

[6] A. Arancibia and K. Strunz. "Modeling of an electric vehicle charging station for fast DC charging," in *2012 IEEE International Electric Vehicle Conf.* pp. 1-6.

[7] A. Rahoui, A. Bechouche, H. Seddiki, and D. O. Abdeslam. "Grid Voltages Estimation for Three-Phase PWM Rectifiers Control Without AC Voltage Sensors," *IEEE Trans. Power Electronics*, vol. 33, pp. 859-875, Jan. 2016.

[8] Y. Liu, T. Wang, Y. Yang and X. Wang. "Modeling and simulation of electric vehicles' charge and discharge system," Power System Protection and Control. China, vol. 42, pp. 70-76, 2014.

[9] A. M. Omara and M. Sleptsov. "Bidirectional interleaved DC/DC converter for electric vehicle application," in *2016 11th International Forum on Strategic Technology*, pp. 100-104.

[10] L. Cao, S. Wu, C. Zhang and B. Wu. "A general method of SPWM harmonic analysis," Power Electronics. China, vol. 36, pp. 62-65, 2002.

[11] J. Liu and Y. Li. "Dead-time influence on output error of voltage source inverter and compensation," Transactions of China Electrotechnical Society. China, vol. 22, pp. 117-122, 2007.